PHYSICAL REVIEW B VOLUME 25, NUMBER 8 15 APRIL 1982

Cyclotron resonance and Shubnikov–de Haas experiments in a *n*-InAs-GaSb superlattice

H. J. A. Bluyssen, J. C. Maan,* and P. Wyder
Research Institute for Materials, University of Nijmegen, Toernooiveld, 6525 ED Nijmegen, The Netherlands

L. L. Chang and L. Esaki
IBM Thomas J. Watson Research Center, Yorktown Heights, New York 10598
(Received 16 June 1981)

Cyclotron resonance is observed in a semiconducting *n*-InAs-GaSb superlattice by measuring the change of the far-infrared-radiation (FIR) transmission in a magnetic field at three different FIR frequencies. The angular dependence of the cyclotron resonance position is measured and shows a two-dimensional behavior. The resonance observed is attributed to an upwards shift of 145 meV of the InAs conduction band as a consequence of the superlattice subband formation. A simple calculation leads to a value of 195 meV for this shift.

I. INTRODUCTION

Superlattices (SL) are layered structures consisting of periodically arranged alternative layers of two different materials with a good lattices match. Layer thicknesses are typically of the order of 10 to 50 times the lattice constant. The superlattice periodicity superimposed on the lattices periodicity leads to a division of the Brillouin zone into subzones with boundaries at wave-vector values $k_z = n\pi/d$ with d the superlattices periodicity, k the superlattices wave vector and n an integer; z is the direction perpendicular to the layers. In the superlattice direction subbands are formed separated by small gaps. Therefore, superlattices have electronic properties which differ markedly from those of the constituent materials.[1,2]

The most remarkable aspect of the SL band structure is its anisotropy. If the layer thicknesses are much larger than the de Broglie wavelength there is no influence of successive layers of the same material on each other. In this case the SL behaves as a purely two-dimensional (2D) material due to the quantum size effect, as long as the energy separation between successive subbands is large compared with the thermal energy kT; if this condition is not fulfilled, a simple three-dimensional (3D) behavior of the individual layers will be observed. For smaller layer thicknesses the interaction between successive layers leads to a more three-dimensional (3D) character of the SL band structure. The degree of dimensionality can be measured by the width of the subband; the smaller the subband width the more the 2D character dominates. In this case the SL can be considered as a set of 2D electron gases. Due to the research done on the metal-oxide semiconductor field-effect transistor, the electronic properties of such systems were studied extensively.[3,4]

Man-made superlattices have become a reality through the development of the molecular-beam epitaxial technique which made it possible to grow layers of a few lattice constants[5,6] with very abrupt interfaces.[1,7,8] Up to now, superlattices have been grown from GaAs, AlAs, InAs, and GaSb, and their alloy compounds. The sample used in the present experiments is made from InAs and GaSb. These SL differ from GaAs-$Ga_xAl_{1-x}As$ SL because the GaSb valence band (VB) is higher in energy than the InAs conduction band (CB), whereas in the former type the band gaps overlap. Band-structure calculations of the InAs-GaSb SL have shown that besides the usual subband formation, a semiconductor-to-semimetal transition occurs[9–11] for layer thicknesses in excess of 100 Å. In addition, the strong energy dependence of the effective masses involved can be used to verify the energy-level structure by a determination of the effective mass by Shubnikov–de Haas[12] and cyclotron resonance[13] measurements.

In this paper, cyclotron resonance (CR) measurements are reported; preliminary results of these studies have been published before.[13] Simple band-structure calculations indicate that the thicknesses of the superlattice layers of the sample under investigation here (65-Å InAs and 80-Å GaSb) lead to a semiconductor (in contrast to a semimetal). On this sample cyclotron resonance measurements are performed as a function of the magnetic field and of the angle between the plane of the SL and the magnetic field using far-infrared radiation at wavelengths λ of 118.8, 70.6, and 57 μm and high magnetic fields (up to 15 T).

From the electronic mass determined by CR with the magnetic field B perpendicular to the SL plane, the subband energy is derived by fitting the observed CR absorption to a theoretical model of the line shape, incorporating nonparabolicity of the conduction band, and interference and plasma effects. CR measurements as a function of the angle between the direction of the magnetic field and the direction perpendicular to the SL plane reveal that, despite the considerable subband width (calculated to be 14 meV, essentially a 2D character of the subbands is observed. From Shubnikov—de Haas measurements and the subband energy obtained from the CR measurements, the Fermi energy is determined experimentally. Good agreement is found with the Fermi energy calculated on basis of a 2D density-of-states function and the experimental determined value of the carrier concentration.

II. InAs-GaSb SUPERLATTICE BAND STRUCTURE

Band structure of superlattices was initially calculated with the one-dimensional, Kronig-Penney model, applied to quasifree electrons with the effective mass of the bulk materials.[14] This procedure gives accurate results for the $Ga_xAl_{1-x}As$-GaAs superlattices, because the band gaps of the two materials overlap, and a simple square-wave-modulated potential for the CB and VB results.

For InAs-GaSb SL, this simple procedure can no longer be applied. From values for the electron affinities of InAs and GaSb it follows that the InAs CB must be 140 meV below the GaSb VB. From analysis of optical data of InAs-GaSb type of superlattices[11] and of I-V characteristics of InAs-GaSb heterojunctions,[15] it is found that for the InAs CB 150 meV below the GaSb VB, the best agreement between theory and experimental data is obtained. Despite these uncertainties in the exact

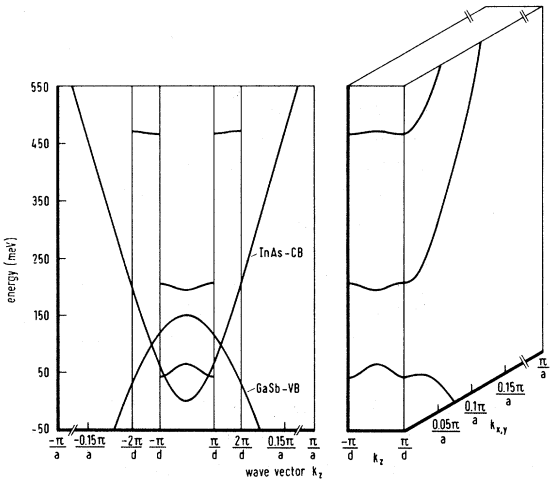

FIG. 1. Band structure of an InAs-GaSb superlattice. The left panel shows how subbands are formed from the original InAs conduction band and the GaSb valence band. The right panel shows the resulting band structure. The calculations were performed for layer thicknesses of 65 Å (InAs) and 80 Å (GaSb); $d = 145$ Å.

band lineup it is clear that these different bands are so close to each other that the simple Kronig-Penney model cannot be applied directly. Two approaches have subsequently been used to calculate the band structure of such superlattices. One is based on a method of linear combination of atomic orbits,[10] the other on the matching at the interfaces of the Bloch wave functions and their spatial derivatives of the basic materials.[9] Using the latter method, the superlattice band structure in the z direction (perpendicular to the layers in the xy plane) has been calculated. The result for the sample used in the present experiments (65-Å InAs, 80-Å GaSb) is shown in Fig. 1. Table I summarizes the sample parameters and the results for the parameters of the band-structure calculation. Band-gap energy values of 0.41 eV for InAs and 0.82 eV for GaSb were used, while the values for the effective mass of the electrons and the light holes were taken as $m_e = 0.023 m_0$ and $m_h = 0.053 m_0$. As mentioned above, the position of the bulk InAs CB was taken as 150 meV below the GaSb VB edge.

As expected the Brillouin zone is divided into subzones with boundaries at $k_z = \pi/d$ and subbands are formed. However, it should be emphasized that while the origin of the subbands in the simple Kronig-Penney model is a potential difference between adjacent materials, here they are caused by the orthogonality of the CB and VB wave functions. Apart from an upwards shift of

TABLE I. Superlattice sample characteristics.

InAs layer thickness	65 Å
GaSb layer thickness	80 Å
Number of periods	125
Carrier concentration (Hall measurement)	4.8×10^{17} cm^{-3}
Carrier mobility (Hall measurement)	7300 cm^2/V s
Subband-edge energy	195 meV
Subband width	14 meV
Calculated Fermi energy (above first subband)	40 meV
Measured Fermi energy (above first subband)	38.4 meV

the CB and a downwards shift of the VB edges with respect to those in InAs and GaSb, respectively, the dispersion relation in the (x,y) direction is not affected by the superlattice configuration. The right panel of Fig. 1 shows the resulting band structure of the superlattice: small subbands in the z direction and the original bulk dispersion relation in the (x,y) direction. Since the superlattice under investigation is doped with donors, one has to concentrate on the lowest conduction subband. In particular, the effect of a magnetic field in the z direction can be calculated in the following way. The original bulk InAs CB in the two-band k-p approximation is given by

$$\frac{\hbar^2}{2m_0^*}(k_x^2+k_y^2+k_z^2)=E\left[1+\frac{E}{E_G}\right], \tag{1}$$

with m_0^* the band-edge effective mass, $\hbar$ Planck's constant, E the energy measured from the band edge, (k_x,k_y,k_z) the wave vectors in InAs, and E_G the band gap of the bulk InAs. In a superlattice the lowest energy occurs for $k_x=k_y=0$, and at a value of k_z dictated by the superlattice periodicity. The energy corresponding to this value is E_1, the shift of the superlattice subband with respect to the InAs band edge. If a magnetic field is applied parallel to the z axes, the term with k_x^2 and k_y^2 has to be replaced by $(N+\frac{1}{2})(\hbar eB/m_0^*)$ due to the Landau quantization. As a result one gets for the energy levels in a magnetic field:

$$(N+\tfrac{1}{2})\frac{\hbar eB}{m_0^*}=E_N\left[\frac{E_N}{E_G}+1\right]-E_1\left[\frac{E_1}{E_G}+1\right], \tag{2}$$

and for the effective mass:

$$m_{x,y}^*(E_1,B)=m_0^*\left[1+\frac{E_{N+1}(E_1,B)+E_N(E_1,B)}{E_G}\right], \tag{3}$$

where m_0^* is the effective mass at the band edge of bulk InAs, and $E_N(E_1,B)$ can be calculated from Eq. (2). The effective mass in the z direction can be derived from the curvature of the calculated E_1 subband, while the effective mass in the (x,y) direction is given by the energy dependence of the effective mass in InAs. Figure 2 shows the results for the effective mass in both directions for the lowest CB of the superlattice under investigation. The mass in the z direction varies from $+0.052$ at the bottom of the subband to -0.07 at the top of the subband and is generally much larger than the

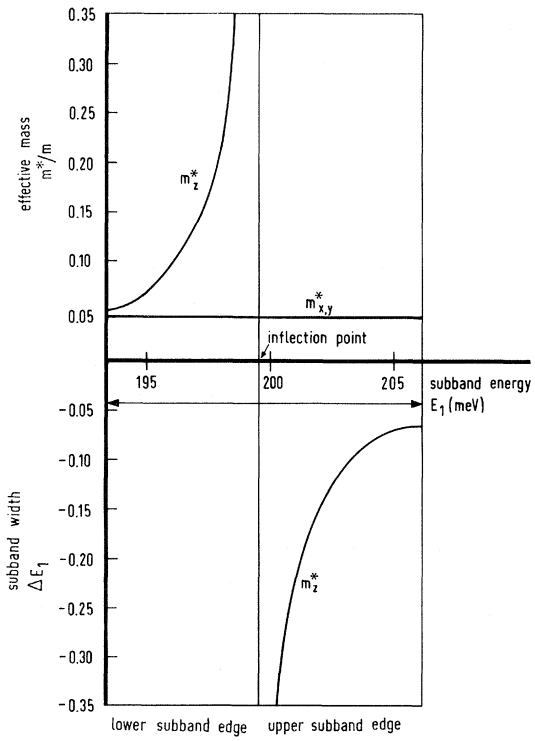

FIG. 2. Anisotropy of the effective mass in the conduction band of a superlattice with layer thicknesses of 65 Å (InAs) and 80 Å (GaSb). m_z^* is calculated numerically from the subband curvature, $m_{x,y}^*$ from the energy dependence of the effective mass in InAs.

effective mass in the (x,y) direction except from a small energy range around $k_z=0$ and $k_z=\pi/d$. The mass in the (x,y) direction is the same as that for bulk InAs, but now taken at an energy E_1, the shift in the InAs CB edge is due to the superlattice structure.

III. EXPERIMENTAL DETAILS

The experimental setup to study cyclotron resonance in a n-InAs-GaSb superlattice is shown in Fig. 3. Far-infrared radiation (FIR) transmission is observed at a fixed frequency as a function of the magnetic field. The radiation is generated with an optically pumped CH_3OH/D FIR laser. Three different wavelengths are used, namely $\lambda=118.8$, 70.6, and 57.8 μm. By dividing the transmission signal with a signal directly obtained from the laser beam, fluctuations in the transmitted signal due to laser instabilities could be drastically reduced. Both signal and reference signal are mechanically chopped at 23 Hz and detected by two He-cooled bolometers using conventional phase-sensitive methods.

The FIR radiation was focussed onto a 5×1 mm exit slit just above the sample with the use of oversized lightpipes (9 mm i.d.). The sample itself was glued to a tablet which could be rotated from the top of the insert, inside a variable temperature cryostat (see Fig. 3). Magnetic fields up to 15 T are generated by a Bitter coil of the Nijmegen High Magnetic Fields Installation.[16] The configuration of the superlattice is shown in Fig. 4 and consists of 125 alternating layers of 65-Å InAs and 80-Å GaSb grown on a planparallel [100]-oriented semi-insulating GaAs substrate by the molecular-beam epitaxial technique.[1,17] To avoid dislocations due to the lattice mismatch of the GaAs substrate with InAs, an insulating 1500-Å transition layer was grown from GaAs to InAs.[17] The lattice mismatch between InAs and GaSb is well below 1% which is better than required for a smooth heteroepitaxial interface. The layer thicknesses were determined from the calibrated growth rates. The electron concentration and the mobility were determined from Hall measurements. The sample was intentionally doped with Sn to obtain the desired carrier concentration. The sample parameters are summarized in Table I.

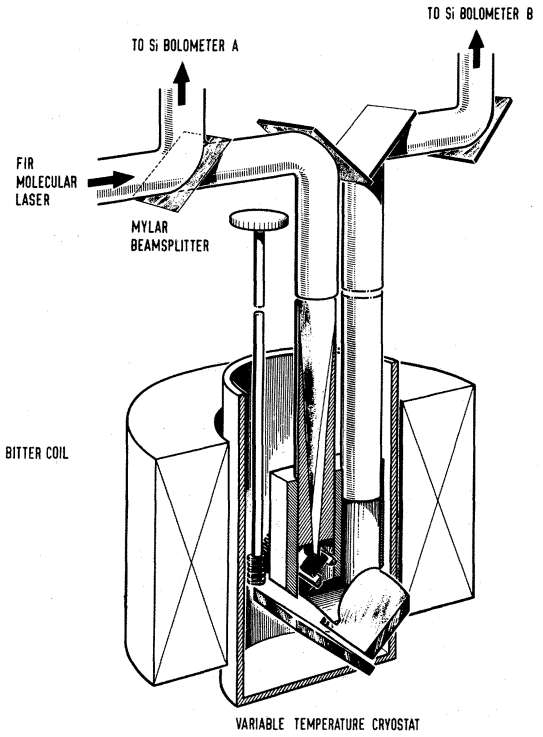

FIG. 3. Experimental setup (schematic).

IV. CYCLOTRON RESONANCE MEASUREMENTS

The FIR transmission of the superlattice as a function of the magnetic field B, for B perpendicular to the superlattice plane, is shown in Fig. 5 for wavelengths of $\lambda=118.8$, 70.6, and 57 μm, respectively. The measurements reveal broad but clearly resolved minima which are interpreted as cyclotron resonance absorption of the electrons in the lowest conduction subband. It is well known from cyclotron resonance measurements on a metal-oxide–semiconductor field effect transistor (MOSFET) that, for a layer carrier density of $10^{11}-10^{12}$ cm^{-2}, which is of the same order as the density in the present sample, the transmission minimum does not necessarily coincide with the position of the resonance[18–20] as a consequence of line-shape distortion by plasma effects and interference ef-

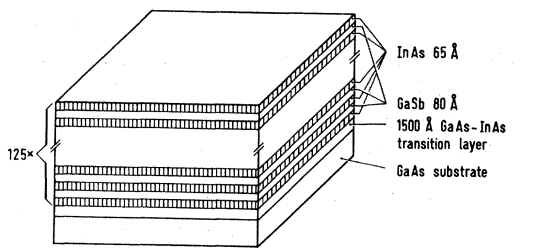

FIG. 4. Configuration of the superlattice.

fects in the parallel substrate. It has been shown that plasma effects in a 2D electron gas become important if $\omega_{ps}\tau \gtrsim 0.15$, where $\omega_{ps}=4\pi n_s e^2/(m^* cn)$, with n_s the layer carrier density, e the electron charge, m^* the effective mass, c the speed of light, and n the refractive index. This condition is not fulfilled in the present experiment and therefore, in the analysis of the line shape, the influence of the flat substrate is dominant. To analyze the data, the electromagnetic properties of the superlattice are approximated by that of a single-layer 2D electron gas on a parallel substrate. This assumption is realistic because the phase of the incident wave will not change significantly for successive layers as the total superlattice thicknesses (2 μm) is much smaller than the wavelength. With this approximation the SL transmission as a function of the magnetic field was calculated by a method previously used for MOSFET's.[18–20] However, it should be noted that while in the case of MOSFET, the effective mass itself is the quantity of interest, here the superlattice effective mass is related to the InAs CB edge effective mass and the energy shift E_1 by Eq. (3).

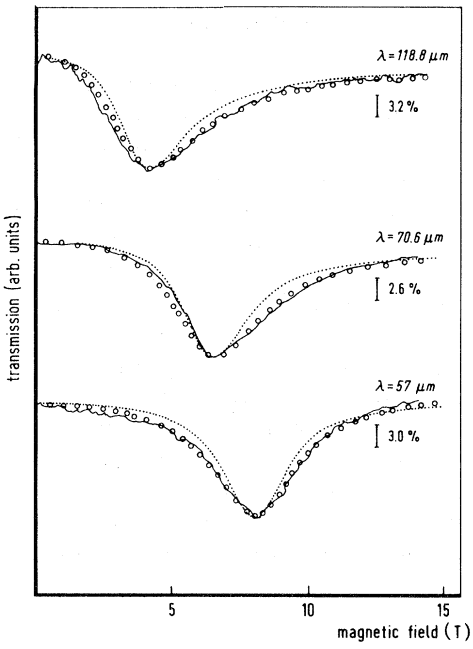

FIG. 5. Measured (solid line) and calculated CR transmission line shapes of an InAs-GaSb superlattice. For the calculations a subband shift of $E_1=145$ meV is used, while the peak transmission and the interference parameter are fitted to the data. The dotted curves are calculated for $E_1=145$ meV, $\tau=1.8\times10^{-13}$ s, and a 14-meV subband width. The circles indicate a fit with a scattering time $\tau=1.4\times10^{-13}$ s.

Therefore, the CR experiment measures indirectly this energy shift E_1.

Owing to the energy dependence of the effective mass as expressed in Eq. (3), the Landau levels E_N and E_{N+1} between which cyclotron absorption takes place have to be specified. The present sample is a degenerate material with a Fermi energy of 40 meV above the subband edge. Since transitions take place between a Landau level below and a Landau level above the Fermi energy, cyclotron resonance absorption may occur between different Landau levels for different magnetic fields as illustrated in Fig. 6. Finally, the third important difference stems from the fact that simple calculations for the present superlattice lead to a subband width of 14 meV, whereas subbands in a MOSFET are flat. This value of 14 meV is of the same order as the Landau-level splitting, and therefore more than two subbands are involved in cyclotron resonance absorption if the Fermi energy intersects one or more subbands, as is also shown in Fig. 6.

To account for all these effects, the SL transmission under cyclotron resonance conditions was calculated in several steps:

(1) For given values of the magnetic field B and the energy shift E_1, the Landau levels E_N are calculated from Eq. (2).

(2) The values for N, E_N, and E_{N+1} of the Landau levels, which are adjacent to the calculated Fermi energy (40 meV above the subband edge), are inserted in Eq. (3) to calculate the effective mass.

(3) This value of the effective mass is used to calculate the transmission from the standard expression for a 2D electron gas with a scattering time τ.[18,19]

(4) To account for the 14-meV subband width, this procedure is repeated for E_1 increased in small steps until $E=E_1+14$ meV, and the results for the transmission are added.

In this way the SL transmission in a magnetic field is calculated for the three frequencies used and these can be compared with the experimental data. The results are shown in Fig. 5. The amplitude of the calculated transmission, the InAs subband shift E_1, and the scattering time τ, are the only adjustable parameters and they are fitted to the experimental data. A very good fit with the experimental results (indicated by the circles in Fig. 5) is obtained with $E_1=145$ meV and $\tau=1.4\times10^{-13}$ s. It should be emphasized that for all three frequencies the same values for E_1 and τ were used.

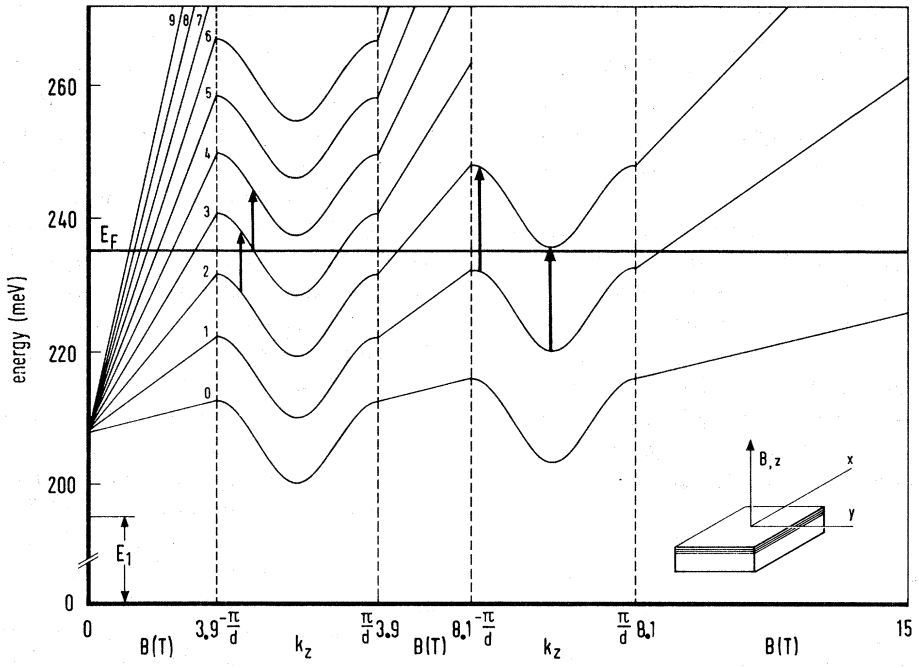

FIG. 6. Calculated splitting of the subband as a function of magnetic field with $E_1=195$ meV and magnetic-field dependence of the subband energy at the Brillouin-zone edge. The arrows indicate transitions from states below the Fermi level to states above the Fermi level and correspond to a different energy spacing due to the energy dependence of the effective mass. This illustrates the influence of the band structure on the CR line shape.

In the preceding discussion no attention has been paid to the spin splitting of the Landau levels which, through the nonparabolicity and the high g factor ($g=-15$),[21] can contribute to the cyclotron resonance line shape.[22,14] For pure InAs, the difference in magnetic fields for the cyclotron resonance transitions between the spin-up and the spin-down Landau levels is about 0.25 T at ~ 8 T, and this difference must be greater than the cyclotron resonance linewidth in order to be observable. This was the case for the pure InAs samples studied in Refs. 21 and 22, but in our case, however, the linewidth is much broader. In addition, the effect of the spin splitting is much smaller due to the energy dependence of the g factor. If this effect should be taken into account in a manner consistent with the two-band model, a term of the form $\pm\frac{1}{2}g\mu_B B$ must be added to the left-hand side of Eq. (2). In this way, the energy difference between the cyclotron resonance transition for the spin-up and the spin-down Landau levels is calculated as 0.1 T at ~ 8 T which is definitely too small to be observable in our situation. Furthermore, it is well known that the two-band model underestimates the energy dependence of the g factor as compared with more elaborate calculations.[21] At the energies of interest in our case (~ 180 meV above the InAs band edge), the g factor is reduced from $g=-15$ to $g=-6.5$ in the two-band model, while more precise calculations[21] predict $g=0$ at 185 meV. Therefore, we believe that the neglect of the spin splitting in the present discussion is justified.

Using the standard formula for the energy dependence of the effective mass in a nonparabolic material, $m^*=m_0^*(1+2E/E_G)$, the mass at zero magnetic field can be calculated for $E=E_1+E_F$ as $0.044m_0$ (m_0 is the electron mass). Using this value and the measured mobility, the scattering time is calculated to be 1.8×10^{-13} s, which is somewhat longer than the one derived from the fitting of the linewidth (1.4×10^{-13} s). For comparison, the fit to the line shape with $\tau=1.8\times10^{-13}$ s is shown as the dotted line in Fig. 5. Both the linewidth and the transport mobility did not vary with temperature between 4 and 40 K.

The experimental value obtained for E_1 ($E_1^{\text{expt}}=145$ meV) is significantly different from the calculated value of 195 meV. The main reason for this discrepancy is probably due to the approximations used in the band-structure calculations for the superlattice. The calculations were restricted to a two-band $\vec{k}\cdot\vec{p}$ model only and, more importantly, the band structure in the superlattice has

only been calculated for $k_x = k_y = 0$, which is incorrect in the presence of a magnetic field. As the value of E_1 is not very sensitive to the difference in energy between the InAs CB and the GaSb VB, taken to be 150 meV, these uncertainties of these relative positions cannot account for the observed discrepancy.

In conclusion, the cyclotron resonance measurements clearly show a significant mass enhancement due to the lifting of the InAs CB by the superlattice periodicity. Within the approximation of the theory used there is a reasonable agreement between the calculated and measured subband shift. In addition, the scattering time derived from the CR linewidth is in fairly good agreement with the one derived from Hall measurements.

V. SHUBNIKOV–de HAAS MEASUREMENTS

Figure 7 gives the derivative of the sample resistance as a function of the magnetic field. This measurement clearly shows oscillations with the typical $1/B$ periodicity as indicated in the inset. These oscillations occur whenever a Landau level crosses the Fermi energy. With the help of Eq. (2) the periodicity of the oscillations $\Delta(1/B)$ can be calculated as

$$\Delta\left[\frac{1}{B}\right] = \frac{\hbar e}{m_0^*}\left[\frac{E_F^2}{E_G} + E_F\left[1+\frac{2E_1}{E_g}\right]\right]^{-1}, \tag{4}$$

where E_F is measured with respect to the first-subband energy, E_1. Using this equation, E_F can be obtained from the measured periodicity, since the subband shift E_1 has already been obtained by the independent measurement of cyclotron resonance. In this way one gets a Fermi energy of 38.5 meV. This value is in fairly good agreement with the calculated value of 40 meV, obtained in the usual way by integration over the density of states until the measured carrier density is obtained. This close agreement justifies the use of 40 meV for the Fermi energy in the fit to the line shape in the preceding section.

Although there is a significant difference between the calculated and measured value of E_1, there is a rather good agreement between the calculated and measured Fermi energy. The reason for this is that both the calculated and measured Fermi energy are measured from the edge of the subband E_1 and not from the bulk InAs CB edge. Therefore, uncertainties in E_1 play only a secondary role through the effective mass which enters in the expression for the density of states.

VI. ANGULAR-DEPENDENCE MEASUREMENTS

Figures 8(a) and 8(b) show the observed transmission of the superlattice as a function of the magnetic field for two wavelengths ($\lambda = 118.8$ and 70.6 μm) for various orientations of the superlattice plane with respect to the magnetic field.

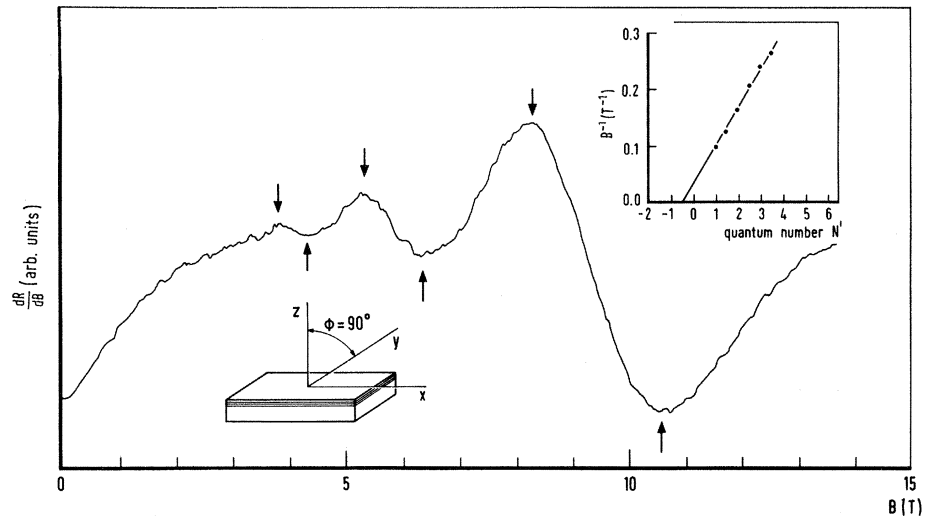

FIG. 7. Shubnikov–de Haas oscillations in the derivative of the superlattice resistance as a function of magnetic field. The inset shows the magnetic field values at which extrema occur (the arrows) as a function of the quantum number N'. Note that N' is not the Landau-level quantum number because extrema in the derivative do not occur at integer Landau-level numbers.

The results show a substantial anisotropy of the cyclotron resonance line, as would indeed be expected from the pronounced anisotropy of the superlattice effective mass shown in Fig. 2.

In Sec. IV a value for the ac-scattering time, $\tau=1.4\times10^{-13}$ s, was derived from the fit to the cyclotron resonance line shape; this time corresponds to a level broadening $\hbar/\tau$ of 5 meV. As can be seen from Fig. 2 the superlattice effective mass in the z direction is small only in a small energy region close to $k_z=0$ and $k_z=\pi/d$. Consequently, the 5-meV level broadening will mask any contribution of this finite effective mass to the angular dependence of the cyclotron resonance, and therefore the transverse mass can be considered to be much larger than the longitudinal one. In this case the angular dependence is simply that of a 2D electron gas, and for the resonance position the following equation holds:

$$B_{\rm res}(\varphi)=B_{\rm res}(\varphi=90°)\sin\varphi\ . \tag{5}$$

Equation (5) is compared with the experimental data in Fig. 8(c) and it can be seen that the experimental results are well described for $\lambda=70.6$ μm and somewhat less well for $\lambda=118.8$ μm. However, as was discussed in Sec. IV, in the present sample the resonance position cannot simply be identified by the minimum in the transmission, due to interference effects and plasma effects. These effects will certainly play an important role in a detailed analysis of the angular dependence as by tilting the sample, due to its high refraction index, the Poynting vector of the radiation outside the sample parallel to the B field (Faraday configuration), will make an angle with the B field inside the sample, leading to a mixture of the Faraday and the Voigt configurations. In addition, for the same reason the path lengths of the radiation inside the sample and the substrate will be different at different angles, leading to different interference conditions. It can be seen from the experimental spectra that these effects do play a role as, especially for $\lambda=118.8$ μm at angles far from 90°, the transmission at high magnetic fields exceeds the zero-field transmission. Simple model calculations of interference and plasma effects[18,19] show that such a behavior is very easily observed under these conditions, and for the parameters of the sample under investigation deviations of the transmission minimum from the resonance position of up to 15% can occur.

VII. CONCLUSIONS

In conclusion, it can be stated that cyclotron resonance is observed in a n-InAs-GaSb superlattice. The resonance position is clearly different from that of the bulk materials and can be related to the band-edge InAs effective mass by taking into account the shift in the InAs CB edge result-

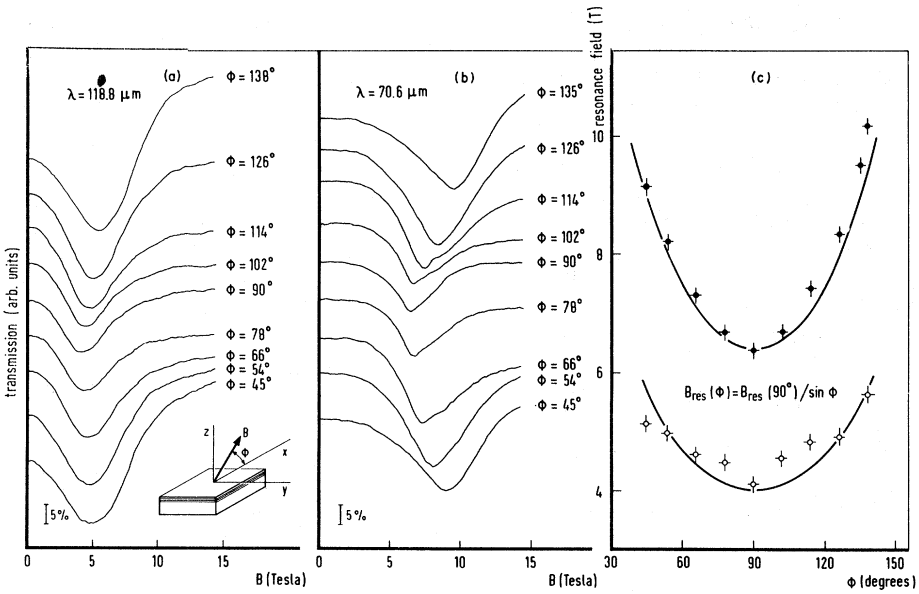

FIG. 8. Angular dependence of the transmission of the superlattice as a function of magnetic field and orientation for $\lambda=118.8$ and 70.6 μm. (c) shows the transmission minima of B plotted against ϕ. The drawn line shows the theoretical angular dependence of a 2D system.

ing from the superlattice periodicity. This band-edge shift is determined from the experimental data as 145 meV. From simple band-structure calculations, using a modified Kronig-Penney model, a value of 195 meV is obtained. The difference is attributed to the fact that in the superlattice band-structure calculations the subband structure is calculated for $k_x = k_y = 0$ only, which is incorrect if a magnetic field is present. Unfortunately, no detailed calculations for the band structure of a superlattice in a magnetic field have yet been performed, and, strictly speaking, all band-structure formulas used in the present paper have to be considered as only rough approximations. In view of these facts there is a reasonable quantitative agreement between measured and calculated values. The position of the Fermi energy is measured with the Shubnikov–de Haas effect to be 38.4 meV, and this value is in good agreement with the 40 meV obtained from integration over the density of states to obtain the measured carrier density. From our analysis of the cyclotron resonance line shape, a value for the scattering time τ of 1.4×10^{-13} s is obtained which is somewhat shorter than the value of 1.8×10^{-13} s as was derived from the dc Hall mobility. Finally, a measurement of the angular dependence of the cyclotron resonance position shows the essentially 2D character of this superlattice.

ACKNOWLEDGMENTS

Part of this work has been supported by the "Stichting voor Fundamenteel Onderzoek der Materie" (FOM), with financial support of the "Nederlandse Organisatie voor Zuiver Wetenschappelijk Onderzoek" (ZWO). The work at the IBM Thomas J. Watson Research Center was partially supported under an Army Research Office Contract.

---

*Present address: Max-Planck Institut für Festkörperforschung, Hochfeld-Magnetlabor, 166 X, F 38042 Grenoble, France.

[1]L. Esaki and L. L. Chang, Thin Solid Films 36, 285 (1976).

[2]R. Dingle, *Festkörperprobleme XV,* edited by H. V. Queisser (Pergamon-Vieweg, Braunschweig, 1975), p. 21.

[3]J. F. Koch, *Festkörperprobleme XV,* edited by H. V. Queisser (Pergamon-Vieweg, Braunschweig, 1975), p. 79.

[4]G. Landwehr, *Festkörperprobleme XV,* edited by H. V. Queisser (Pergamon-Vieweg, Braunschweig, 1975), p. 49.

[5]L. L. Chang, L. Esaki, W. E. Howard, R. Ludeke, and G. Schul, J. Vac. Sci. Technol. 10, 655 (1973).

[6]R. Dingle, W. Wiegman, and G. H. Henry, Phys. Rev. Lett. 33, 827 (1974).

[7]L. L. Chang, A. Segmüller, and L. Esaki, Appl. Phys. Lett. 28, 39 (1976).

[8]R. Ludeke, L. Esaki, and L. L. Chang, Appl. Phys. Lett. 24, 417 (1976).

[9]G. A. Sai Halasz, R. Tsu, and L. Esaki, Appl. Phys. Lett. 30, 651 (1977).

[10]G. A. Sai Halasz, L. Esaki, and W. A. Harrison, Phys. Rev. B 18, 2812 (1978).

[11]G. A. Sai Halasz, L. L. Chang, J. M. Welter, C. A. Chang, and L. Esaki, Solid State Commun. 27, 935 (1978); L. L. Chang, N. Kawai, G. A. Sai Halasz, R. Ludeke, and L. Esaki, Appl. Phys. Lett. 35, 939 (1979).

[12]H. Sakaki, L. L. Chang, G. A. Sai Halasz, C. A. Chang, and L. Esaki, Solid State Commun. 26, 589 (1978).

[13]H. Bluyssen, J. C. Maan, P. Wyder, L. L. Chang, and L. Esaki, Solid State Commun. 31, 35 (1979).

[14]L. Esaki and R. Tsu, IBM J. Res. Dev. 14, 61 (1970).

[15]H. Sakaki, L. L. Chang, R. Ludeke, C. A. Chang, G. A. Sai Halasz, and L. Esaki, Appl. Phys. Lett. 31, 211 (1977).

[16]K. van Hulst, C. J. M. Aarts, A. R. de Vroomen, and P. Wyder, J. Magn. Magn. Mater. 11, 317 (1979).

[17]C. A. Chang, R. Ludeke, L. L. Chang, and L. Esaki, Appl. Phys. Lett. 31, 759 (1977).

[18]J. A. Kennedy, R. J. Wagner, B. D. McCombe, and J. J. Quinn, Solid State Commun. 18, 275 (1976).

[19]M. V. Ortenberg, Solid State Commun. 17, 1335 (1975).

[20]G. Abstreiter, J. P. Kotthaus, J. F. Koch, and G. Dorda, Phys. Rev. B 14, 2480 (1976).

[21]C. R. Pidgeon, D. L. Mitchell, and R. N. Brown, Phys. Rev. 154, 737 (1967).

[22]C. W. Litton, R. B. Dennis, and S. D. Smith, J. Phys. C 2, 2146 (1969).